**Crosstalk between Nrf2 and YAP contributes to maintaining the antioxidant potential and chemoresistance in bladder cancer**

**Crosstalk between Nrf2 and YAP contributes to maintaining the antioxidant potential and chemoresistance in bladder cancer.**

**Running Title:** Nrf2 and YAP crosstalk in cancer chemoresistance.

Ciamporcero Eric*[1,4], Daga Martina[1]*, Pizzimenti Stefania[1]*, Roetto Antonella[1], Dianzani Chiara[3], Compagnone Alessandra[4], Palmieri Antonietta[1], Ullio Chiara[1], Luigi Cangemi[3], Pili Roberto[4,5], Barrera Giuseppina[1].

1.Department of Clinical and Biological Sciences, University of Turin, Corso Raffaello 30, 10125 Turin (CE, DM, PS, UC BG), and Regione Gonzole 10, 10043 Orbassano (Turin) (RA, PA), Italy

2. Department of Drug Science and Technology, University of Turin, Via Pietro Giuria 9, 10125 Turin, Italy

3. Department of Oncology, University of Turin, Via Michelangelo 27, 10125 Turin, Italy

4. Department of Medicine, Genitourinary Program, Roswell Park Cancer Institute, Elm & Carlton Streets, Buffalo, NY 14263, USA.

5. Genitourinary Program, Indiana University-Simon Cancer Center, Hematology/Oncology 980 W. Walnut Street R3 C516, Indianapolis, IN 46202, USA.

*These Authors contributed equally to this work.

**Correspondence to:** Stefania Pizzimenti; Department of Clinical and Biological Sciences, University of Turin; Corso Raffaello 30, 10125 Torino, Italy; Fax +39-011-6707753; **e-mail**: stefania.pizzimenti@unito.it

**Abstract**

Redox adaptation plays an important role in cancer cells drug resistance. The antioxidant response is principally mediated by the transcription factor Nrf2, that induces the transcriptional activation of several genes involved in GSH synthesis, chemoresistance, and cytoprotection. YAP is emerging as a key mediator of chemoresistance in a variety of cancers, but its role in controlling the antioxidant status of the cells is yet elusive. Here, we show that impairing YAP protein expression reduced GSH content and Nrf2 protein and mRNA expression in bladder cancer cells. Moreover, in YAP- knockdown cells the expression of FOXM1, a transcription factor involved in Nrf2 transcription, was down-regulated and the silencing of FOXM1 reduced Nrf2 expression. On the other hand, the silencing of Nrf2, as well as the depletion of GSH by BSO treatment, inhibited YAP expression, suggesting that cross-talk exists between YAP and Nrf2 proteins. Importantly, we found that silencing either YAP or Nrf2 enhanced sensitivity of bladder cancer cells to cytotoxic agents and reduced their migration. Furthermore, the inhibition of both YAP and Nrf2 expressions significantly increased cytotoxic drug sensitivity and synergistically reduced the migration of chemoresistant bladder cancer cells. These findings provide a rationale for targeting these transcriptional regulators in patients with chemoresistant bladder cancer, expressing high YAP and bearing a proficient antioxidant system.

**Keywords:** Glutathione, Nrf2, YAP, FOXM1, chemoresistance, bladder cancer cells

## Introduction

Redox status is a well-recognized actor in the adaptation of cancer cells to therapy [1]. Several types of cancer cells display a large amount of reactive oxygen species (ROS), due to an aberrant metabolism, mitochondrial dysfunction or activation of oncogenes [2]. This characteristic makes cancer cells more vulnerable to damage by further ROS production induced by cytotoxic therapeutic agents, such as cisplatin or doxorubicin, which trigger oxidative stress by binding to cytoplasmic nucleophilic species, including glutathione (GSH), and other cysteine-rich proteins, and induce cancer cell senescence and death [3]. However, some cancer cells, in particular those in advanced stages of disease, become highly adapted to intrinsic or drug-induced oxidative stress by up-regulating their GSH antioxidant system [3]. The transcription factor Nrf2 (NF-E2-related factor 2) is the master regulator of antioxidant and cytoprotective systems. Under physiological conditions, Nrf2 localizes in the cytoplasm where it is bound by Keap1 (Kelch-like ECH-associated protein 1). Keap1 forms a complex with Cul3 and Rbx1, and this E3 ubiquitin ligase complex is able to bind and ubiquitinate Nrf2, resulting in Nrf2 proteasomal degradation [4]. Cellular oxidative stress triggers the oxidation of certain cysteine residues of Keap1, resulting in a conformational change of the Keap1ï Nrf2 complex which prevents Nrf2 ubiquitination [4]. The stabilized Nrf2 accumulates in nuclei, heterodimerizes with small Maf proteins and activates target genes for cytoprotection through the antioxidant response element (ARE)/electrophile response element (EpRE) [5]. A Nrf2 role in chemoresistance has been demonstrated in diverse type of cancers, including cisplatin-resistant bladder cancers [6-8].

Among the several genes involved in chemoresistance, increasing evidence has demonstrated the involvement of Yes-associated protein (YAP) in drug resistance of diverse types of cancers. YAP is a key component of the Hippo tumor-suppressor pathway [9], and Hippo pathway-mediated YAP phosphorylation on Ser127 mainly leads to its cytoplasmic sequestration or ubiquitination and degradation [10]. Conversely, non-phosphorylated YAP translocates into the nucleus where it binds to transcription factors (mainly from TEAD family), triggering the expression of several genes involved in organ size control, cell proliferation and survival [11]. Indeed, inhibition of YAP expression results in reduced cell proliferation and enhanced cell death through modulation of downstream transcriptional targets [12]. YAP expression and nuclear localization strongly correlate with poor patient outcome and the progression of several tumors, including bladder cancer [12-15]. Recently, we demonstrated that constitutive expression and activation of YAP inversely correlated with ñ*in vitro*ò and ñ*in vivo*ò cisplatin

sensitivity of urothelial cell carcinoma cells [16]. YAP overexpression protects, while YAP knockdown sensitizes cancer cells to chemotherapy and radiation effects via increased accumulation of DNA damage and apoptosis [16]. Through the usage of an alternative transcription factor (FoxO1), YAP has also been linked to antioxidant balance maintenance in cardiomyocytes: YAP stimulation prevents, whereas YAP down-regulation promotes oxidative stress-induced cell death [17]. YAP binding to the transcription factor FoxO1 could form a functional complex on the promoters of antioxidant genes such as catalase and MnSOD, stimulating their transcription [17]. Recently, also the interaction with Pitx2 has been proposed as a mechanism for the YAP inducing antioxidant response in cardiomyocytes [18]. Interestingly, in this model, YAP cooperated with Nrf2 to sustain the antioxidant response, suggesting a functional crosstalk between the two pathways. Moreover, YAP expression is regulated, among the others, by a redox-dependent transcription factor: GABP, an Ets family member. Indeed, acetaminophen-induced GSH depletion inhibits GABP transcriptional activity and depletes YAP [19]. These data reiterate that a positive feedback loop between YAP and Nrf2 antioxidant system could exist. Indeed, the increase in antioxidant defenses could induce YAP expression, which in turn could promote the synthesis of antioxidant genes. Although a direct link between YAP and Nrf2 expression has not yet been proven, it can be argued by considering the regulation of forkhead box M1 (FOXM1) expression. This transcription factor is associated with a variety of aggressive solid carcinomas, including bladder cancer [20], and it is involved in the regulation of several genes, including Nrf2 [21]. It has been recently reported that YAP/TEAD regulates FOXM1 expression [22], thus, through this pathway YAP could affect Nrf2 expression.

Although the role of Nrf2 and YAP in chemoresistance and in maintenance of the antioxidant cellular level has been demonstrated, no data are available in regards to a possible crosstalk between these two pathways in chemoresistant cancer cells which display high antioxidant level. In this study, we report that induction of cisplatin resistance in bladder cancer cells can affect the expression and function of Nrf2 and YAP and that the inhibition of YAP expression can interfere with the expression of Nrf2 and vice-versa, rescuing the sensitivity to chemotherapy.

## Materials and methods

*Cells and culture conditions*

253J and 253J B-V cell lines were kindly provided by Dr Colin Dinney (MD Anderson Cancer Center). Human UCC cell line T24 was purchased from ATCC (Manassas, VA, USA).
These cells were cultured in RPMI 1640, supplemented with 10% FBS, 100 units per ml penicillin and 100ε g/ml streptomycin in a 5% CO 2, 37°C incubator.

*Induction of cisplatin resistance*

Resistance to cisplatin (CDDP) was induced by exposure of 253J and 253J B-V cells to progressively higher concentrations of CDDP (0.5-0.8-1-1.3-1.5 ε g / ml). CDDP resistant cell lines were generated in Dr. Piliôs laboratory. Each concentration was maintained for at least 6 weeks and the viability of the resistant phenotype was verified. After this period, the cells remained for at least one month in the absence of drug; when a recovery of proliferation was observed, the drug concentration was increased to the higher dose. The induction of resistance to the highest drug concentration required a year. The acquired resistance was analyzed by MTT and colony forming assays.

*MTT assay*

The toxic effect of CDDP was determined through the 3-(4,5-dimethyl thiazol-2-yl)-2,5-diphenyltetrazolium bromide (MTT) assay. This is a colorimetric assay used to determine the level of metabolic activity in cells able to reduce the yellow tetrazolium dye MTT to purple formazan crystals. The amount of formazan produced an indication of the mitochondrial integrity and activity, which, in turn, may be interpreted as a measure of both cell viability and cell proliferation [23]. MTT analysis was performed in 96-well plates. Cells were seeded (800ï 1500 cells/well) in 200 ε l of serum-supplemented medium and treated with different CDDP concentrations. Untreated cells were used as control. After this period, the drug was removed and MTT assay was performed. MTT was added to control and treated cells to a final concentration of 0.5 mg/ml (Sigmaï Aldrich) for 2 hours. The medium was then removed, and the cells were lysed with 100 ε l of DMSO. Absorbance was recorded at 530 nm by a 96-well-plate ELISA reader.

*Crystal violet assay*

The viability of cells after CDDP treatment was detected through the staining with crystal violet dye, which binds to proteins and DNA. The amount of crystal violet staining depends on the

amount of adherent cells, where cells that undergo cell death lose their adherence and are subsequently lost from the cell population, reducing the amount of crystal violet staining in the well [24]. The crystal violet assay was determined as described by Feoktistova et al (2016) [24].

*Colony-forming assay*

Cells were trypsinized, washed in 1×PBS, and seeded (500 cells/well) into a six-well plate and left overnight to attach. After 24 h, the cells were treated with the compounds and the medium was changed after 72 h. Cells were cultured for 9ï 11 days and subsequently ýxed and stained with a solution of 90% crystal violet (Sigmaï Aldrich), 10% methanol. The colonies were then photographed and counted with a Gel Doc equipment (Bio-Rad Laboratories).

*Analysis of GSH and GSSG contents*

GSH and GSSG contents were determined by the Owens and Belcher method [25] by using 2 $x10^6$ cells for each condition and reported as a GSH/GSSG ratio.

*Lysate preparation and western blot analysis*

Cells were seeded in75-cm2 þasks and treated as indicated. Subsequently, the cells were harvested, washed once in ice-cold 1×PBS; resuspended in a lysis buffer composed of 20 mM Trisï HCl, pH 7.4, 150 mM NaCl, 5 mM EDTA, 1% v/v Triton X-100, phosphatase (Sigmaï Aldrich P2850), and protease (Sigmaï Aldrich P8340) inhibitor cocktails; and incubated for 15 min at 4 °C. Samples were centrifuged at 10,000 rpm for 15 min at 4 °C, the supernatants were collected, and the protein concentration was determined using a commercially available kit (Bio-Rad Laboratories). Western blot analysis was performed using home-made 9.3% SDSï polyacrylamide gels or 5ï 15% gradient SDSï polyacrylamide precast gels (Bio-Rad Laboratories). Twenty to 40ε g of proteins was mixed with 20ε l of Laemmli sample buffer (Bio-Rad Laboratories 161-0737) containing 10% 2-mercaptoethanol, boiled for5 min, and loaded onto the gels. The run was performed at the constant voltage of 100 V. The proteins were then transferred onto a nitrocellulose membrane with a semidry transfer apparatus (Biometra). The membranes were subsequently blocked for 1 h with 5% nonfat dry milk dissolved in TBSï Tween 20, incubated overnight at 4 °C with primary antibodies, washed three times with TBSï Tween 20, and incubated with HRP-conjugated secondary antibodies for 1 h at room temperature. Antibodies used were as follows: PARP (#9542), Asp214 cleaved PARP (#9541) glyceraldehyde 3 phosphate dehydrogenase (GAPDH) (#5174) (Cell Signaling, Boston, MA, USA); ϐ-actin (sc-47778), YAP (sc15407), Nrf2 (sc 722), Keap-1 (sc33569), FOXM1 (sc 271746) (Santa Cruz, Dallas, TX, USA); Ŭ-tubulin (04-1117, Millipore, Billerica, MA, USA);

thioredoxin (H00007295-M01) (Novus Biologicals, Milano, Italy); glutathione-S-transferase A4 (SAB1401164) (Sigmaï Aldrich). The detection of the bands was carried out after reaction with chemiluminescence reagents (PerkinElmer NEL105001EA) through ýlm (Santa Cruz Biotechnology sc-201697) autoradiography.

*Immunofluorescence*

Cells ($5x10^4$) were plated into the channels of a µï Slide VI0.4 (Ibidi, Giemme Snc, Milano, Italy). After treatments, cells were fixed for 15 min in 4% paraformaldehyde and permeabilized with 1% Triton X-100 for 30 min at room temperature and washed with PBS. Then, the slides were incubated with 1% BSA in 1x PBS for 30 min at room temperature, after which they were incubated for 1 h at room temperature with the primary monoclonal antibody against YAP (D8H1X, Cell Signaling, Boston, MA, USA) or Nrf2 (D179C, Cell Signaling, Boston, MA, USA) in 1% BSA dissolved in PBS. The cells were subsequently washed, incubated for 1 h at room temperature with the secondary FITC-conjugated antibody (1:100 in 0.1%BSA in 1x PBS). After washing with PBS, the cells were analyzed under a fluorescence microscope (Axiovert 35; Carl Zeiss MicroImaging GmbH, Jena, Germany).

*RNA interference*

Expression arrest pGIPZ lentiviral vector encoding non-silencing control shRNA or YAP1 shRNAs (V2LHS_65508 and V2LHS_65509, Thermo Scientiýc Open Biosystems, Waltham, MA, USA) were provided as described before [16]. Virus supernatant was applied with 8ε g/ml polybrene on 60ï 70% conþuent cells and non-infected cells were eliminated through puromycin selection. In siRNA experiments, $2 \times 10^4$ 253J C-r cells and T24 cells were seeded in 12-well plates in medium containing serum and antibiotics and transfected with 50 nM Nrf2-specific siRNA (SI 03246950; Qiagen) or FOXM1 specific RNA (sc-43769, Santa Cruz Biotechnology), using the HiPerfect transfection reagent (Qiagen) according to the manufacturer's instructions.

*BSO treatment*

253J C-r cells and T24 cells were seeded in 12-well plates in medium containing serum and antibiotics and treated with 100 or 200µM Buthionine-sulfoximine (BSO) (Sigmaï Aldrich) for 24, 48 and 72 hours.

*Quantitative reverse transcription polymerase chain reaction (qRT-PCR)*

For reverse transcription, 1 εg of cells total RNA, 25 μM random hexamers and 100 U of Reverse Transcriptase (Thermo Fisher Scientific, USA) were used. Gene expression levels were measured by quantitative real time PCR (qRT-PCR) in an iCycler (Bio-Rad Laboratories, USA). Abelson (Abl) gene was utilized as housekeeping controls. The following TaqMan® Gene Expression Assay (Thermo Fisher Scientific, USA) were used: Hs00975960_m1 for Nrf2 gene; Hs00371735_m1, Life Technologies for YAP gene and Hs00245445_m1 for Abl gene,g respectively. For each PCR reaction, 50 ng of cDNA was added to PCR reaction mix containing 1x TaqMan Universal PCR Master Mix (Thermo Fisher Scientific, USA), 1x TaqMan® Gene Expression Assay (Thermo Fisher Scientific, USA) and distilled water to a final volume of 10 ul. All analyses were carried out in duplicate; results showing a discrepancy greater than one cycle threshold in one of the wells were excluded. The results were analyzed using the qpqpCt method [26].

*Apoptosis*

Adherent and nonadherent cells where harvested, washed in 1 × PBS, and subsequently resuspended in annexin V binding buffer (556454; BD Pharmingen) supplemented with 1:100 APC-conjugated annexin V (550474; BD Pharmingen) and 1 εg/ml propidium iodide (Sigmaï Aldrich). Cells were analyzed by a FACSCalibur cytometer (Becton Dickinson).

*Wound Healing Assay*

In the scratch assay, after starvation for 18ï 24 h in serum-free medium, cells were plated onto six-well plates (106 cell/well) and grown to confluence. Cell monolayers were wounded by scratching with a pipette tip along the diameter of the well, and they were washed twice with serum-free medium. In order to monitor cell movement into the wounded area, five fields of each wound were photographed immediately after the scratch (0 h) and after 24 h [27-28]. The endpoint of the assay was measured by calculating the reduction in the width of the wound after 24 h and compared to 0 h which is set at 100%. The area of wound healing was calculated by using the ImageJ software [29].

*Statistical analysis*

Data were expressed as means ± SD. Significance between experimental groups was determined by one-way ANOVA followed by the Bonferroni multiple comparison post-test using GraphPad InStat software (San Diego, CA, USA). Values of pÒ0.05 were considered statistically significant.

**Results**

*Induction of cisplatin resistance*

To analyze the role played by YAP and Nrf2 in CDDP resistance of human bladder cancers, we exposed 253J and 253J B-V bladder cancer cells to increasing CDDP concentrations for 12 months. Resistance induction was demonstrated by MTT assay and colony forming assay (Supplementary data Fig.1). Indeed, the ability to grow, as well as to form colonies, indicated that these cell lines were made resistant to cisplatin and thus labeled as 253J C-r and 253J B-V C-r (CDDP-resistant). Figure 1 shows the results obtained by the evaluation of GSH/GSSG ratio (Figure 1A), and the expression of YAP, Nrf2, and Nrf2 target genes: heme oxygenase 1 (HO-1), thioredoxin (Trx) and gluatathione-S-transferase A4 (GSTA4) (Figure 1 B and C). In both cell lines, the acquired resistance induced an upregulation of YAP and Nrf2 expressions, accompanied by an increase of GSH/GSSG ratio. Accordingly with Nrf2 increase, HO-1 and GSTA4 were upregulated in the resistant lines, whereas Trx displayed a different expression and appeared upregulated only in resistant 253J cells. In 253J C-r cells the GSH/GSSG ratio was higher than that observed in 253J B-V C-r cells. Thus, 253J and 253J C-r cells were chosen for the following experiments.

*YAP down-regulation sensitized 253J cells to chemotherapeutic agents and reduced Nrf2 expression.*

To evaluate the role of YAP in CDDP resistance in 253J cells, we modulated its expression and examined the response to CDDP treatment. 253J C-r cells were infected with either YAPsh RNAs (labeled as YAPsh) or a non-silencing control shRNA (labeled as NSsh) expressing pGIPZ lentiviral vector. YAP level in these cells was analyzed by western blot (Fig 2 A) and immunofluorescence (Fig. 2 B) confirming that YAP shRNA significantly reduces YAP expression in 253J C-r cells. PARP cleavage was used as an indicator of apoptosis induction in a CDDP dose-response experiment in 253J C-r NSsh and 253J C-r YAPsh cells (Fig. 2 C). YAP knockdown makes cancer cells more sensitive not only toward CDDP, but also toward other DNA damage-inducing agents, such as camptothecin (CPT), doxorubicin (DOX) and gemcitabine (GEM) (Fig. 2 D). Quantification of cleaved PARP, performed by densitometric scanning and related to the representative western blots (Fig. 2 panels C and D) is shown in Fig. 2 panel E. These results were in agreement with previous data obtained in our laboratory on T24 human bladder cancer cells [16].

To test the hypothesis of whether YAP has a critical role in controlling the antioxidant potential of the cells, we evaluated the GSH/GSSG ratio and Nrf2 expression in 253J C-r NSsh and 253J C-r YAPsh cells. In YAP knocked down cells both the GSH/GSSG ratio (Fig. 3A) and Nrf2 protein (Fig. 3 B and C) were decreased, indicating that YAP can play a role in the control of this cellular antioxidant system.

The reduction of Nrf2 protein expression could depend on the intracellular level of Keap1, which binds and drives Nrf2 to proteasomal degradation, or on a reduction of Nrf2 mRNA synthesis. To investigate the cause of the reduction of Nrf2 protein expression in YAP knocked down cells, we first analyzed Keap1 expression in 253J C-r NSsh and 253J C-r YAPsh (Fig. 3 D). Keap1 expression was not modified in YAP knocked down 253J C-r cells with respect to the 253J C-r NSsh cells, and this suggested that the reduction of Nrf2 protein did not depend on Keap1 targeting. On the contrary, the Nrf2 mRNA expression, detected through qRT-PCR varied significantly (Fig. 3 E). In particular, Nrf2 mRNA expression paralleled with its protein expression, being also higher in resistant cells than in sensitive cells, according to the up-regulation of YAP expression, and reduced in YAPsh cells with respect to NSsh cells. These results suggested that YAP action on Nrf2 expression was at the transcriptional level.

Since previous literature data indicated that YAP-TEAD can modulate FOXM1 expression [22] which, in turn, can control Nrf2 expression [21] we analyzed FOXM1 expression in our exclusive models (Fig.4 A). Results demonstrated that FOXM1 is upregulated in resistant cells and this increase was lost by knocking down YAP in these cells. Moreover, to confirm an involvement of FOXM1transcription factor in Nrf2 expression regulation, we silenced FOXM1 through a specific siRNA in 253J C-r cells (Fig. 4B) and evaluated the Nrf2 mRNA expression in 253J C-r and in 253J C-r Nrf2 silenced cells. Results obtained demonstrated that the silencing of FOXM1 reduced the expression of Nrf2 mRNA (Fig. 4 C).

*Nrf2 silencing reduced YAP expression and sensitized 253J cells to CDDP treatment.*

Since it has been demonstrated that a depletion of antioxidant species can result in a reduction of YAP expression [19], we assessed whether the silencing of Nrf2, the master regulator of the antioxidant potential, could produce a reduction of YAP expression. To test this hypothesis, 253J C-r cells were transient silenced for Nrf2 using a specific siRNA. The peak of silencing was reached 24 hours after siRNA transfection (Fig. 5A). Subsequently, the level of Nrf2 expression gradually increased and returned to the control values within 3 days (data not shown). At 24 hours, the expression of YAP was reduced in Nrf2 silenced cells with respect to control 253J C-r cells (Fig. 5B). Immunofluorescence staining confirmed the reduction of YAP protein expression 24 hours after siRNA transfection (Fig. 5C). Moreover, we examined the YAP mRNA expression and detected a significant reduction in Nrf2 silenced cells (Fig. 5D). It has been reported that the oxidation of the Ets family member GABP, which binds to the Yap promoter and activates YAP transcription [19], can be inactivated by oxidative mechanisms and by glutathione depletion [19]. To confirm that a reduction of cell antioxidant defenses could reduce YAP expression, we analyzed

YAP mRNA expression in 253J C-r cells in which GSH was depleted by BSO. Analogously to that observed in Nrf2 silenced cells, the BSO treatment reduced the YAP mRNA expression (Fig. 5D). To verify whether the silencing of Nrf2 or the BSO treatment could increase the sensitivity toward CDDP treatment, the response to a toxic concentration of CDDP was analyzed in 253J C-r and 253J C-r Nrf2 silenced cells in terms of crystal violet assay and apoptosis detection through cytofluorimetric analysis (Fig. 5 E and F). Results obtained demonstrated that Nrf2 silencing significantly reduced cell viability 24, 48 and 72 hours after treatment with 5 μM CDDP and increased by about 3 fold the number of apoptotic cells 24 hours after treatment with 20 μg/ml CDDP. The reduction of viability in BSO treated cells was similar to that observed in Nrf2 silenced cells (Fig. 5 E)

*YAP or Nrf2 knocking downs influence the reciprocal expression and sensitize T24 cells to CDDP treatment.*

To verify whether a crosstalk between YAP and Nrf2 is also present in another cell line from the same origin, we examined the expression of Nrf2 and HO-1 genes in YAP knocked down T24 cells (T24 YAPsh) and YAP expression in Nrf2 silenced cells (T24 siNrf2). We previously demonstrated that T24 cells display high levels of YAP expression and a high resistance to CDDP treatments, which was lost in YAP knocked-down cells (T24 YAPsh) [16]. Results obtained in T24YAPsh cells demonstrated that in these cells the Nrf2 expression was decreased, as well as the expression of Nrf2 target gene HO-1 (Fig. 6A). According to that observed in 253J C-r YAPsh cells, in T24 YAPsh cells the GSH/GSSS ratio was reduced (Fig. 6B) and the Nrf2 silencing reduced YAP expression (Fig. 6C). Interestingly, in YAPsh cells also silenced for Nrf2, the inhibition of Nrf2 expression was even more evident (Fig. 6D). Moreover crystal violet assay demonstrated that the silencing of YAP and/or Nrf2 expressions or BSO treatment increased the sensitivity to CDDP treatment (Fig. 6E).

*The down-regulation of both YAP and Nrf2 increased CDDP sensitivity and reduced 253J migration.*

The reduction of Nrf2 expression was analyzed in 253J C-r, 253J C-r silenced for Nrf2, 253J C-r YAPsh cells and in YAPsh cells silenced for Nrf2. The reduction of Nrf2 expression in YAPsh cells silenced for Nrf2 was higher than that observed in Nrf2 silenced cells 48 hour after transfection. (Fig. 7A). Concomitant down-regulation of Nrf2 and YAP produced a higher sensitivity toward CDDP-induced inhibition of proliferation than that observed after altering one of these proteins at a time (Fig. 7B). Moreover, 24 hours after a treatment with 20 μg/ml CDDP, the number of apoptotic

cells after the inhibition of both proteins was higher than that observed in single Nrf2 silenced cells or in YAP knocked down cells (Fig. 7C).

A well-established YAP role on physiological cellular behavior, is its action on cell migration which is related in oncology field to the invasion and the metastatic capability of tumor cells [30-32]. In addition, some data indicated that Nrf2 suppression also reduced the migration in different tumor cells [33-34]. To verify whether the reduction of YAP and/or Nrf2 expressions could reduce cell migration, we analyzed this parameter through the wound healing method in Nrf2 silenced, YAP knocked down cells and in cells silenced for both genes (Fig. 8). We observed that 253J resistant cells were able to migrate faster than the sensitive ones and that silencing YAP or Nrf2 reduced the migration of resistant cells. Interestingly, concomitant silencing of YAP and Nrf2 can rescue the migration phenotype observed in sensitive cells, indicating that the down-regulation of these genes had a synergic effect in the inhibition of cell migration.

**Discussion**

The ability of the tumor cells to develop resistance to chemotherapy remains a major challenge in the management of urothelial cancer patients. Among the factors involved in chemoresistance, the redox adaptation and the increase in detoxifying molecules play an important role in apoptosis evasion of chemoresistant cells [35]. GSH is a major player in intracellular redox adaptation and is involved in several metabolic pathways, cell cycle progression and antioxidant defenses [36]. Our results suggest that the induced resistance to cisplatin in human bladder cancer cells is accompanied by an increase of the intracellular level of GSH. Similar results were obtained by Iida et al. which demonstrated an increase of gamma-glutamylcysteine synthetase expression and intracellular GSH levels in doxorubicin- or cisplatin-resistant human cancer cells compared to sensitive cancer cells [37].

The main enzymes involved in GSH synthesis and utilization are controlled by the transcription factor Nrf2 [38]. Consequently, the Nrf2 overexpression is associated with the increase of GSH in chemoresistant cells [39]. Our results in bladder cancer cells show a substantial increase in Nrf2 expression after induction of CDDP resistance. Moreover, we demonstrated that Nrf2 silencing resensitized chemotherapy resistant cells to CDDP treatment. It has been reported that Nrf2 induces the transcriptional activation of more than 100 detoxification and cytoprotective genes [40], including several genes involving in chemoresistance, such as ABCF2 [41], Xct [42], and Glutathione S-transferases [43]. Moreover, Nrf2 upregulates the transcription of Bcl-2 and Bcl-xL antiapoptotic genes [44, 45], thus Nrf2 down regulation may make cancer cells more prone to apoptosis.

Recently, YAP role in chemoresistance of several tumors, including bladder cancer, has emerged [16]. In our cellular model, the induction of CDDP resistance caused an upregulation of YAP expression, and YAP silencing increased the sensitivity of bladder cancer cells not only toward CDDP, but also toward other DNA damaging agents, in agreement with our previous observations performed in bladder cancers [16]. However, the molecular mechanisms of YAP action, have not been completely elucidated. Through TEAD interaction YAP controls a set of genes such as CTGF, cyr61, survivin, amphiregulin and AXL [11, 14, 46], and some of them have been associated with drug resistance [47]. However, YAP role in controlling the antioxidant defense of chemoresistant cancer cells has not yet been reported. Our results suggest that YAP upregulation in chemoresistant cells is accompanied by an increase in the GSH/GSSG ratio and Nrf2 expression and, more importantly, that YAP knockdown reduced the GSH/GSSG ratio and Nrf2 expression, thus indicating a direct contribution of YAP in regulating the antioxidant potential of cancer cells. The reduction of the GSH/GSSG ratio and Nrf2 expression have been confirmed in another urothelial cell line: T24 cells, which displayed high chemoresistance accompanied by a high level of YAP expression [16]. YAP involvement in redox regulation has been reported by Shao et al. in cardiomyocytes in which the effect of YAP-FOXO1 interaction and FOXO1-dependent induction of anti-oxidant proteins, SOD2 and catalase, counteracted ROS-induced cellular senescence [17]. Our results broaden the spectrum of antioxidant activity exerted by YAP, since it could also be linked to a regulation of Nrf2 expression, and, consequently, of its target antioxidant genes. The demonstration that the YAP-knocking down reduced the Nrf2 mRNA indicated that YAP control on Nrf2 expression was at the transcriptional level. Since there was not a direct involvement of YAP in the activation of transcription factors which regulated Nrf2 transcription, we postulated an indirect action involving FOXM1 transcription factor. The FOXM1 transcription factor plays a crucial role in regulating cell proliferation, differentiation, and transformation. Overexpression of FOXM1 is associated with a variety of aggressive solid carcinomas, including bladder cancer [12], and it has been related to the drug resistance in a variety of cancers [48-50].

FOXM1 is a downstream target of YAP, which directly induces FOXM1 transcription in a TEAD-dependent fashion [22]. On the other hand, it has been recently demonstrated that Nrf2 is transcriptionally activated by FOXM1 [21]. This observation suggests that YAP may affect Nrf2 transcription through the regulation of FOXM1 expression. Our results demonstrate that FOXM1 expression is increased in resistant cells, and that YAP knocking down highly inhibits FOXM1 protein expression. Moreover, FOXM1 silencing reduced Nrf2 expression, thus suggesting a role for FOXM1 in YAP-mediated Nrf2 regulation.

Interestingly, the silencing of Nrf2 also inhibited YAP expression in both 253J C-r and T24 cells, suggesting a bidirectional cross-talk between these two molecules. YAP expression inhibition could depend on the reduction of Nrf2-controlled antioxidant genes, such as HO-1 and others, with consequent oxidation of the Ets family member GABP, which binds to the Yap promoter and activates YAP transcription [19]. Indeed, it has been reported that GABP can be inactivated by oxidative mechanisms and by glutathione depletion [19], both mechanisms linked to Nrf2 activity. The involvement of an oxidative inactivation of GABP in our cell model was also confirmed by the observation that YAP mRNA was significantly inhibited in GSH depleted 253J C-r cells after BSO treatment.

Based on these observations, by sustaining the antioxidant potential of the cell, YAP supports its expression. In addition, the reduction of antioxidants, by Nrf2 inhibition or BSO treatment, may result in GABP inactivation and, consequently, in a YAP expression inhibition. Moreover, the silencing of Nrf2 in YAP knocked down cells, resulted in a stronger reduction of Nrf2 expression and in an increase of CDDP sensitivity compared to the cells silenced only for Nrf2 or for YAP.

In addition to the induction of apoptosis, YAP and Nrf2 also control the migration of cancer cells [33-34, 51], which contributes to metastatic properties of cancer cells. Our results also show a reduction of migration in Nrf2 silenced and YAP knocked down- CDDP-resistant bladder cells and a greater inhibitory effect in Nrf2 silenced- YAP knocked down cells.

## Conclusions

Our results suggest that both Nrf2 and YAP are involved in maintaining the antioxidant potential of bladder cancer cells and that a bidirectional cross-talk exists between these two jpathway. Moreover, we found that the inhibition of both YAP and Nrf2 expression significantly increased the CDDP sensitivity, by reducing cell viability, increasing apoptosis induction, and inhibiting the migratory capability in chemoresistant bladder cancer cells. These findings provide a rationale for targeting these transcriptional regulators in patients with chemoresistant bladder cancer, expressing high YAP and antioxidant levels.

## Acknowledgements

This work was supported by the University of Turin (Local Funds ex-60% to SP, AR, CD, GP).

## References

[1] Rebucci, M.; Michiels, C. Molecular aspects of cancer cell resistance to chemotherapy. Biochem. Pharmacol. 85: 1219-1226; 2013. doi: 10.1016/j.bcp.2013.02.017.

[2] Pelicano, H.; Carney, D.; Huang, P. ROS stress in cancer cells and therapeutic implications. Drug. Resist. Updat. **7**: 97-110; 2004.

[3] Trachootham, D.; Alexandre, J.; Huang, P. Targeting cancer cells by ROS-mediated mechanisms: a radical therapeutic approach? Nat. Rev. Drug Discov. 8: 579-591; 2009. doi: 10.1038/nrd2803.

[4] Taguchi, K.; Motohashi, H.; Yamamoto, M. Molecular mechanisms of the Keap1ï Nrf2 pathway in stress response and cancer evolution. Genes Cells 16: 123-140; 2011. doi: 10.1111/j.1365-2443.2010.01473.x.

[5] Itoh, K.; Tong, K.I.; Yamamoto, M. Molecular mechanism activating Nrf2-Keap1 pathway in regulation of adaptive response to electrophiles. Free Radic. Biol. Med. 36: 1208-1213; 2004.

[6] No, J.H.; Kim, Y.B.; Song, Y.S. Targeting nrf2 signaling to combat chemoresistance. *J* Cancer Prev. 19: 111-117; 2014. doi: 10.15430/JCP.2014.19.2.111.

[7] Hayden, A.; Douglas, J.; Sommerlad, M.; Andrews, L.; Gould, K.; Hussain, S.; Thomas, G.J.; Packham, G.; Crabb, S.J. The Nrf2 transcription factor contributes to resistance to cisplatin in bladder cancer. Urol. Oncol. 32: 806-814; 2014. doi: 10.1016/j.urolonc.2014.02.006.

[8] van der Wijst, M.G.; Brown, R.; Rots, M.G. Nrf2, the master redox switch: the Achilles' heel of ovarian cancer? Biochim. Biophys. Acta 1846: 494-509; 2014. doi: 10.1016/j.bbcan.2014.09.004.

[9] Harvey, K.F.; Zhang, X.; Thomas, D.M. The Hippo pathway and human cancer. Nat. Rev. Cancer 13: 246-257; 2013. doi: 10.1038/nrc3458.

[10] Zhao, B.; Li, L.; Tumaneng, K.; Wang, C.Y.; Guan, K.L. A coordinated phosphorylation by Lats and CK1 regulates YAP stability through SCF (beta-TRCP). Genes Dev. 24: 72-85; 2010. doi: 10.1101/gad.1843810.

[11] Zhao, B.; Ye, X.; Yu, J.; Li, L.; Li, W.; Li, S.; Yu, J.; Lin, J.D.; Wang, C.Y.; Chinnaiyan, A.M.; Lai, Z.C.; Guan, K.L. TEAD mediates YAP-dependent gene induction and growth control. Genes Dev. 22: 1962-1971; 2008. doi: 10.1101/gad.1664408.

[12] Liu, J.Y.; Li, Y.H.; Lin, H.X.; Liao, Y.J.; Mai, S.J.; Liu, Z.W.; Zhang, Z.L.; Jiang, L.J.; Zhang, J.X.; Kung, H.F.; Zeng, Y.X.; Zhou, F.J.; Xie, D. Overexpression of YAP 1 contributes to progressive features and poor prognosis of human urothelial carcinoma of the bladder. BMC Cancer 13: 349; 2013. doi: 10.1186/1471-2407-13-349.

[13] Steinhardt, A.A.; Gayyed, M.F.; Klein, A.P.; Dong, J.; Maitra, A.; Pan, D.; Montgomery, E.A.; Anders, R.A. Expression of Yes-associated protein in common solid tumors. Hum. Pathol. 39: 1582-1589; 2008. doi: 10.1016/j.humpath.2008.04.012.

[14] Xu, M.Z.; Yao, T.J.; Lee, N.P.; Ng, I.O.; Chan, Y.T.; Zender, L.; Lowe, S.W.; Poon, R.T.; Luk, J.M. Yes-associated protein is an independent prognostic marker in hepatocellular carcinoma. Cancer 115: 4576-4585; 2009. doi: 10.1002/cncr.24495.

[15] Wang, Y; Dong, Q; Zhang, Q; Li, Z; Wang, E; Qiu, X. Overexpression of yes-associated protein contributes to progression and poor prognosis of non-small-cell lung cancer. Cancer Sci. 101: 1279-1285; 2010. doi: 10.1111/j.1349-7006.2010.01511.x.

[16] Ciamporcero, E; Shen, H; Ramakrishnan, S; Yu, K.S.; Chintala, S.; Shen, L.; Adelaiye, R.; Miles, K.M.; Ullio, C.; Pizzimenti, S.; Daga, M.; Azabdaftari, G.; Attwood, K.; Johnson, C.; Zhang, J.; Barrera, G.; Pili, R. YAP activation protects urothelial cell carcinoma from treatment-induced DNA damage. Oncogene 35: 1541-1553; 2016. doi: 10.1038/onc.2015.219.

[17] Shao, D.; Zhai, P.; Del Re, D.P.; Sciarretta, S.; Yabuta, N.; Nojima, H.; Lim, D.S.; Pan, D.; Sadoshima, J. A functional interaction between Hippo-YAP signalling and FoxO1 mediates the oxidative stress response. Nat. Commun. 5: 3315; 2014. doi: 10.1038/ncomms4315.

[18] Tao, G.; Kahr, P.C.; Morikawa, Y.; Zhang, M.; Rahmani, M.; Heallen, T.R.; Li, L.; Sun, Z.; Olson, E.N.; Amendt, B.A.; Martin, J.F. Pitx2 promotes heart repair by activating the antioxidant response after cardiac injury. Nature 534: 119-123; 2016. doi: 10.1038/nature17959.

[19] Wu, H.; Xiao, Y.; Zhang, S.; Ji, S.; Wei, L.; Fan, F.; Geng, J.; Tian, J.; Sun, X.; Qin, F.; Jin, C.; Lin, J.; Yin, Z.Y.; Zhang, T.; Luo, L.; Li, Y.; Song, S.; Lin, S.C.; Deng, X.; Camargo, F.; Avruch, J.; Chen, L.; Zhou, D. The Ets transcription factor GABP is a component of the hippo pathway essential for growth and antioxidant defense. Cell. Rep. 3: 1663-1677; 2013. doi: 10.1016/j.celrep.2013.04.020.

[20] Liu, D.; Zhang, Z.; Kong, C.Z. High FOXM1 expression was associated with bladder carcinogenesis. Tumour Biol. 34: 1131-1138; 2013. doi: 10.1007/s13277-013-0654-x.

[21] Han, B.; Shin, H.J.; Bak, I,S.; Bak, Y.; Jeong, Y.L.; Kwon, T.; Park, Y.H.; Sun, H.N.; Kim, C.H.; Yu, D.Y. Peroxiredoxin I is important for cancer-cell survival in Ras-induced hepatic tumorigenesis. Oncotarget 7: 68044-68056; 2016. doi: 10.18632/oncotarget.11172.

[22] Fan, Q.; Cai, Q.; Xu, Y. FOXM1 is a downstream target of LPA and YAP oncogenic signaling pathways in high grade serous ovarian cancer. Oncotarget 6: 27688-27699, 2015; doi: 10.18632/oncotarget.4280.

[23] Sylvester, P.W. Optimization of the tetrazolium dye (MTT) colorimetric assay for cellular growth and viability. Methods Mol Biol 716: 157-168; 2011. doi: 10.1007/978-1-61779-012-6_9.

[24] Feoktistova, M.; Geserick, P.; Leverkus, M. Crystal Violet Assay for Determining Viability of Cultured Cells. Cold Spring Harb Protoc. 2016(4): pdb.prot087379; 2016.

[25] Owens, C.W.; Belcher, R.V. A colorimetric micro-method for the determination of glutathione. Biochem. J. 94: 705-711; 1965.

[26] Livak, K.J.; Schmittgen, T.D. Analysis of relative gene expression data using real-time quantitative PCR and the 22DDCT Method. Methods 25: 402-408; 2001.

[27] Dianzani, C.; Minelli, R.; Gigliotti, C.L.; Occhipinti, S.; Giovarelli, M.; Conti, L.; Boggio, E.; Shivakumar, Y.; Baldanzi, G.; Malacarne, V.; Orilieri, E.; Cappellano, G.; Fantozzi, R.; Sblattero, D.; Yagi, J.; Rojo, J.M.; Chiocchetti, A.; Dianzani, U. B7h triggering inhibits the migration of tumor cell lines. J. Immunol. ***192***: 4921-4931; 2014. doi: 10.4049/jimmunol.1300587.

[28] Gigliotti, C.L.; Minelli, R.; Cavalli, R.; Occhipinti, S.; Barrera, G.; Pizzimenti, S.; Cappellano, G.; Boggio, E.; Conti, L.; Fantozzi, R.; Giovarelli, M.; Trotta, F.; Dianzani, U.; Dianzani, C. In vitro and in vivo therapeutic evaluation of camptothecin-encapsulated ß-cyclodextrin nanosponges in prostate cancer. J. Biomed. Nanotechnol. 12: 114-127; 2016.

[29] Schneider, C.A.; Rasband, W.S.; Eliceiri, K.W. NIH Image to ImageJ: 25 years of image analysis. Nat. Methods 9: 671-675; 2012.

[30] Yang, S.; Zhang, L.; Purohit, V.; Shukla, S.K.; Chen, X.; Yu, F.; Fu, K.; Chen, Y.; Solheim, J.; Singh, P.K.; Song, W.; Dong, J. Active YAP promotes pancreatic cancer cell motility, invasion and tumorigenesis in a mitotic phosphorylation-dependent manner through LPAR3. Oncotarget 6: 36019-36031; 2015. doi: 10.18632/oncotarget.5935.

[31] Lee, M.J.; Ran Byun, M.; Furutani-Seiki, M.; Hong, J.H.; Jung, H.S. YAP and TAZ regulate skin wound healing. J. Invest. Dermatol. 134: 518-525; 2014. doi: 10.1038/jid.2013.339.

[32] Zhou, X.; Su, J.; Feng, S.; Wang, L.; Yin, X.; Yan J.; Wang, Z. Antitumor activity of curcumin is involved in down-regulation of YAP/TAZ expression in pancreatic cancer cells. Oncotarget 7: 79076-79088; 2016. doi: 10.18632/oncotarget.12596.

[33] Zhao, Q.; Mao, A.; Guo, R.; Zhang, L.; Yan, J.; Sun, C.; Tang, J.; Ye, Y.; Zhang, Y.; Zhang, H. Suppression of radiation-induced migration of non-small cell lung cancer through inhibition of Nrf2-Notch Axis. Oncotarget 8: 36603-36613; 2017. doi:10.18632/oncotarget.16622.

[34] Xue, D.; Zhou, C.; Shi, Y.; Lu, H., Xu, R.; He, X. Nuclear transcription factor Nrf2 suppresses prostate cancer cells growth and migration through upregulating ferroportin. Oncotarget 7: 78804-78812; 2016. doi: 10.18632/oncotarget.12860.

[35] Landriscina, M.; Maddalena, F.; Laudiero, G.; Esposito, F. Adaptation to oxidative stress, chemoresistance, and cell survival. Antioxid Redox Signal 11: 2701-2716; 2009. doi: 10.1089/ars.2009.2692.

[36] Sies, H. Glutathione and its role in cellular functions. Free Radic. Biol. Med. 27: 916-921;1999.

[37] Iida, T.; Mori, E.; Mori, K.; Goto, S.; Urata, Y.; Oka, M.; Kohno, S.; Kondo, T. Co-expression of gamma-glutamylcysteine synthetase sub-units in response to cisplatin and doxorubicin in human cancer cells. Int J Cancer 82: 405-411; 1999.

[38] Gorrini, C.; Harris, I.S.; Mak, T.W. Modulation of oxidative stress as an anticancer strategy. Nat. Rev. Drug Discov. 12: 931-947; 2013. doi: 10.1038/nrd4002.

[39] Wang, X.J.; Sun, Z.; Villeneuve, N.F.; Zhang, S.; Zhao, F.; Li, Y.; Chen, W.; Yi, X.; Zheng, W.; Wondrak, G.T.; Wong, P.K.; Zhang, D.D. Nrf2 enhances resistance of cancer cells to chemotherapeutic drugs, the dark side of Nrf2. Carcinogenesis 29: 1235-1243; 2008. doi: 10.1093/carcin/bgn095.

[40] Jeddi, F.; Soozangar, N.; Sadeghi, M.R.; Somi, M.H.; Samadi, N. () Contradictory roles of Nrf2/Keap1 signaling pathway in cancer prevention/promotion and chemoresistance. DNA Repair (Amst) 54: 13-21; 2017. doi: 10.1016/j.dnarep.2017.03.008.

[41] Bao, L.; Wu, J.; Dodson, M.; Rojo de la Vega, E.M.; Ning, Y.; Zhang, Z.; Yao, M.; Zhang, D.D.; Xu, C.; Yi, X. ABCF2, an Nrf2 target gene, contributes to cisplatin resistance in ovarian cancer cells. Mol. Carcinog. 56: 1543-1553; 2017. doi: 10.1002/mc.22615.

[42] Ye, P.; Mimura, J.; Okada, T.; Sato, H.; Liu, T.; Maruyama, A.; Ohyama, C.; Itoh, K. Nrf2- and ATF4-dependent upregulation of xCT modulates the sensitivity of T24 bladder carcinoma cells to proteasome inhibition. Mol. Cell. Biol. 34: 3421-3434; 2014. doi: 10.1128/MCB.00221-14.

[43] Bai, X.; Chen, Y.; Hou, X.; Huang, M.; Jin, J. Emerging role of NRF2 in chemoresistance by regulating drug-metabolizing enzymes and efflux transporters. Drug Metab. Rev. 48: 541-567; 2016. doi: 10.1080/03602532.2016.1197239

[44] Niture, S.K doi: Jaiswal, A.K. Nrf2 protein up-regulates antiapoptotic protein Bcl-2 and prevents cellular apoptosis. J. Biol. Chem. 287: 9873-9886; 2012. doi: 10.1074/jbc.M111.312694.

[45] Niture, S.K doi: Jaiswal, A.K. Nrf2-induced antiapoptotic Bcl-xL protein enhances cell survival and drug resistance. Free Radic. Biol. Med. 57: 119-131; 2013. doi: 10.1016/j.freeradbiomed.2012.12.014.

[46] Zhang, J.; Ji, J.Y.; Yu, M.; Overholtzer, M.; Smolen, G.A.; Wang, R.; Brugge, J.S.; Dyson, N.J.; Haber, D.A. YAP-dependent induction of amphiregulin identiýes a non-cell-autonomous component of the Hippo pathway. Nature Cell Biol. 11: 1444-1450; 2009. doi: 10.1038/ncb1993.

[47] Reichert, S.; Rodel, C.; Mirsch, J.; Harter, P.N.; Tomicic, M.T.; Mittelbronn, M.; Kaina, B.; Rödel, F. Survivin inhibition and DNA double-strand break repair: a molecular mechanism to overcome radioresistance in glioblastoma. Radiother. Oncol. 101: 51-58; 2011. doi: 10.1016/j.radonc.2011.06.037.

[48] Liu, Y.; Chen, X.; Gu, Y.; Zhu, L.; Qian, Y.; Pei, D.; Zhang, W.; Shu, Y. FOXM1 overexpression is associated with cisplatin resistance in non-small cell lung cancer and mediates sensitivity to cisplatin in A549 cells via the JNK/mitochondrial pathway. Neoplasma 62: 61-71; 2015.

[49] Xie, T.; Geng, J.; Wang, Y.; Wang, L.; Huang, M.; Chen, J.; Zhang, K.; Xue, L.; Liu, X.; Mao, X.; Chen, Y.; Wang, Q.; Dai, T.; Ren, L.; Yu, H.; Wang, R.; Chen, L.; Chen, C.; Chu, X. FOXM1 evokes 5-fluorouracil resistance in colorectal cancer depending on ABCC10. Oncotarget 8: 8574-8589; 2017. doi: 10.18632/oncotarget.14351.

[50] Chiu, W.T.; Huang, Y.F.; Tsai, H.Y.; Chen, C.C.; Chang, C.H.; Huang, S.C.; Hsu, K.F.; Chou, C.Y. FOXM1 confers to epithelial-mesenchymal transition, stemness and chemoresistance in epithelial ovarian carcinoma cells. Oncotarget 6: 2349-2365; 2015. doi: 10.18632/oncotarget.2957.

[51] Li, S.; Yu, Z.; Chen, S.S.; Li, F.; Lei, C.Y.; Chen, X.X.; Bao, J.M.; Luo, Y.; Lin, G.Z.; Pang, S.Y.; Tan, W.L. () The YAP1 oncogene contributes to bladder cancer cell proliferation and migration by regulating the H19 long noncoding RNA. Urol. Oncol. 33: 427.e1-10; 2015. doi: 10.1016/j.urolonc.2015.06.003.

**Figure legendes**

**Figure 1**: **Analysis of the GSH/GSSG ratio and Western blot of YAP, Nrf2, HO-1, Trx, GSTA4 expressions in wild type and CDDP-resistant cells. A:** GSH/GSSG ratio was evaluated in wild-type (wt) 253J and 253J B-V cells and after induction of CDDP resistance (253J C-r and 253J B-V C-r). Values are the mean ± SD of 3 separate evaluations; ** p-value Ò0.01 vs. wild type cells. **B**: Western blot analysis of YAP, Nrf2, HO-1, Trx, and GSTA4 expressions in 253J, 253J C-r, 253J B-V and 253 J B-V C-r cells. Equal protein loading was confirmed by exposure of the membranes to the anti-ß-actin antibody. **C**: Quantification of protein products was performed by densitometric scanning. Data were normalized using the ß -actin signal and are indicated as the mean ± SD from three independent experiments. ** p-value Ò0.01 and * p-value Ò0.05 vs. wild type cells.

**Figure 2: YAP knockdown and response to chemotherapeutic drugs of YAP-knockdown cells**. **A**: 253J C-r cells were infected and stably selected with YAP shRNA (YAPsh) or a non-silencing shRNA (NSsh) expressing pGIPZ lentiviral vector. Knockdown conýrmation was showed in selected cells by western blot analysis. Lower side: densitometric scanning of the bands. Data are normalized using the ß -actin signal and are indicated as the mean ± SD from three independent experiments. ** p-value Ò**0.01** vs. 253J C-r YAPsh. **B**: immunofluorescence microscopy of 253J C-r, 253J NSsh and 253J YAPsh cells stained with anti-YAP antibody and with the secondary fluorescein isothiocyanate (FITC)-conjugated antibody. **C:** Western blot analysis of apoptosis markers PARP and cleaved PARP (cl. PARP) in 253J C-r NSsh and 253J C-r YAPsh cells treated with 1.5 and 3 µg/ml of CDDP. **D**: Western blot analysis of apoptosis markers PARP and PARP cleavage in 253J C-r NSsh and 253J C-r YAPsh cells treated with 1 and 5µM camptothecin (CPT), 2 µg/ml of doxorubicin (DOXO) and 2 µM gemcitabine (GEM). Ŭ-tubulin served as loading control. **E:** Quantification of cl. PARP performed by densitometric scanning and related to the representative western blots showed in Fig 2C and 2D. Data were normalized using the tubulin signal and are indicated as the mean ± SD from three independent experiments. * p-value Ò0.05 vs. NSsh, ** p-value Ò0.01 vs. NSsh.

**Figure 3: YAP knockdown reduced the GSHGSSG ratio and Nrf2 expression. A:** GSH/GSSG ratio evaluated in 253J C-r NSsh and 253J C-r YAPsh cells. Values are the mean ± SD of 3 separate evaluations. ** p-value Ò0.01 vs. 253J C-r NSsh cells. **B**: Western blot analysis of Nrf2 expression in 253J C-r wild type (wt), 253J C-r YAPsh cells and 253J C-r NSsh. Quantification of protein products was performed by densitometric scanning. Data were normalized using the ß -actin signal and are indicated as the mean ± SD from three independent experiments. ** p-value Ò0.01 vs. 253J C-r YAPsh cells. **C:** immunofluorescence microscopy of 253J C-r, 253J C-r NSsh and 253J C-r YAPsh cells stained with anti-Nrf2 antibody and with the secondary fluorescein isothiocyanate (FITC)-conjugated antibody. **D**: Western blot analysis of Keap-1 expression in 253J C-r NSsh and 253J C-r YAPsh cells; Quantification of protein products was performed by densitometric scanning. Data were normalized using the ß -actin signal and are indicated as the mean ± SD from three independent experiments. **E:** Quantitative reverse transcription polymerase chain reaction (qRT-PCR) of Nrf2 mRNA. Abelson (Abl) gene was utilized as housekeeping controls. All analyses were carried out in duplicate; results showing a discrepancy greater than one cycle threshold in one of the

wells were excluded. The results were analyzed using the qpqCt method. ** p-value Ò0.01 vs. 253J C-r NSsh cells.

**Figure 4**. **FOXM1 expression in resistant and YAPsh cells and Nrf2 expression in FOXM1 - silenced cells. A:** Western blot analysis of FOXM1 expression in 253J, 253J C-r NSsh and 253J C-r YAPsh cells; lower side: quantification of protein products was performed by densitometric scanning (lower side). Data were normalized using the ß -actin signal and are indicated as the mean ± SD from three independent experiments. ** p-value Ò0.01 vs. 253J C-r NSsh cells. **B:** Western blot analysis of FOXM1 expression in 253J C-r (Control, Ctrl), 253J C-r siFOXM1 cells, at 24 and 48 hours after transfection; lower side: densitometric scanning of bands. Data were normalized using the ß -actin signal and are indicated as the mean ± SD from three independent experiments. ** p-value Ò0.01 vs. untransfected cells. **C**: Nrf2 mRNA expression in 253J C-r (Control, Ctrl), 253J C-r siFOXM1 cells 48 hours after transfection evaluated by quantitative reverse transcription polymerase chain reaction (qRT-PCR). Abelson (Abl) gene was utilized as housekeeping controls. All analyses were carried out in duplicate; results showing a discrepancy greater than one cycle threshold in one of the wells were excluded. The results were analyzed using the qpqCt method. * p-value Ò0.05 vs. 253J C-r NSsh cells.

**Figure 5. Nrf2 silencing reduced YAP expression and increased CDDP toxicity. A:** Western blot analysis of Nrf2 expression in 253J C-r untransfected cells (Control, Ctrl) or 253J C-r cells transfected with 50 nM Nrf2-specific siRNA (siNrf2), analyzed 12 and 24 hours after transfection; right side: densitometric scanning of bands. Data were normalized using the ß -actin signal and are indicated as the mean ± SD from three independent experiments. * p-value Ò0.05 and ** p-value Ò0.01 vs. untransfected cells. **B**: Western blot analysis of YAP expression in 253J C-r, 253J C-r, and siNrf2 cells, at 24 hours after transfection; **C**: immunofluorescence microscopy of 253J C-r and 253J C-r Nrf2 siRNA cells stained with anti-YAP antibody and with the secondary fluorescein isothiocyanate (FITC)-conjugated antibody. **D:** YAP mRNA expression in 253J C-r cells silenced for Nrf2 and in cells treated with BSO evaluated by quantitative reverse transcription polymerase chain reaction (qRT-PCR). Abelson (Abl) gene was utilized as housekeeping controls. All analyses were carried out in duplicate; results showing a discrepancy greater than one cycle threshold in one of the wells were excluded. The results were analyzed using the qpqCt method. ** p-value Ò0.01 vs. 253J C-r cells. **E:** Crystal violet assay performed in 253J, 253J C-r, 253J C-r siNrf2 cells and 253J C-r cells treated with 200µM BSO, analyzed 24, 48 and 72 hours after the treatment with 5µg/ml of CDDP. Results were expressed as percent of control values and are the mean ± SD of 3 separate experiments;. ** p-value Ò0.01 vs. 253J C-r cells. **F:** Cytofluorimetric analysis of apoptosis in 253J C-r untreated, and 253J C-r and 253J C-r siNrf2 cells, 24 hours after the treatment with 20 µg/ml of CDDP. Results are expressed as percent of annexin V-positive cells and are the mean ± SD from three independent experiments. ** p-value Ò0.01 vs. 253J C-r cells, §§ p-value Ò0.01 vs. 253J C-r CDDP.

**Figure 6**: **YAP or Nrf2 knocking down influenced the reciprocal expression and sensitized T24 cells to CDDP treatment. A**: Western blot analysis of YAP, Nrf2, HO-1, in T24 NSsh and T24 YAPsh. Equal protein loading was confirmed by exposure of the membranes to the anti-ß-actin antibody. Right side: Quantification of protein products performed by densitometric scanning. Data

are normalized using GADPH or ß -actin signal and are indicated as the mean ± SD from three independent experiments. ** p-value Ò0.01 vs. T24 NSsh cells. **B:** the GSH/GSSG ratio was evaluated in T24 NSsh and T24 YAPsh cells. Values are the mean ± SD of 3 separate evaluations; ** p-value Ò0.01 vs. T24 NSsh cells. **C**: Western blot analysis of YAP and Nrf2 in T24 wild type cells (T24 wt) and T24 wt cells transfected with 50 nM Nrf2-specific siRNA (T24 wt siNrf2). Equal protein loading was confirmed by exposure of the membranes to the anti-ß-actin antibody. Right side: quantification of protein products performed by densitometric scanning. Data were normalized using the ß -actin signal and are indicated as the mean ± SD from three independent experiments. ** p-value Ò0.01 vs**.** T24 wt cells. **D:** Western blot analysis of Nrf2 in T24 NSsh and T24 YAPsh cells untreated (control, Ctrl) and transfected with 50 nM Nrf2-specific siRNA (siNrf2). Equal protein loading was confirmed by exposure of the membranes to the anti-ß-actin antibody. Lower side: Quantification of protein products performed by densitometric scanning. Data were normalized using the ß -actin signal and are indicated as the mean ± SD from three independent experiments. ** p-value Ò0.01 vs. untreated control cells. **E:** Crystal violet assay was performed in T24 NSsh, T24 NSsh siNrf2, T24 NSsh treated with 100 µM BSO (BSO), T24 YAPsh and T24 YAPsh siNrf2 at 24, 48 and 72 hours after the treatment with 5µg/ml of CDDP. Results were expressed as percent of control values and are the mean ± SD of 3 separate experiments. *p-value Ò0.05 and ** p-value Ò0.01 vs. T24 NSsh; § p-value Ò0.05 and §§ p-value Ò0.01 vs. T24 YAPsh.

**Figure 7. The down-regulation of both Nrf2 and YAP increased CDDP toxicity. A:** Western blot analysis of Nrf2 expression in 253J C-r, 253J C-r siNrf2, 253J C-r YAPsh and 253J C-r YAPsh-siNrf2 cells, 48 after transfection; right side: Quantification of protein products performed by densitometric scanning. Data were normalized using the ß -actin signal and are indicated as the mean ± SD from three independent experiments. ** p-value Ò0.01 vs. 253J C-r, §§ p-value Ò0.01 vs. 253J C-r siNrf2 and ÒÒp-value Ò0.01 vs 253J YAPsh-siNrf2.
**B:** Crystal violet assay was performed in 253J C-r NSsh, 253J C-r NSsh siNrf2, 253J C-r YAPsh, 253J C-r YAPsh siNrf2 cells, at 24, 48 and 72 hours after the treatment with 5µg/ml of CDDP. Results were expressed as percent of control values and are the mean ± SD of 3 separate experiments. *p-value Ò0.05 and ** p-value Ò0.01 vs. 253J C-r NSsh cells, §p-value Ò0.05 and §§ p-value Ò0.01 vs. 253J C-r YAPsh. **C**: cytofluorimetric analysis of apoptosis in 253J C-r NSsh, 253J C-r NSsh siNrf2, 253J C-r YAPsh, 253J C-r YAPsh siNrf2 cells, 24 hours after the treatment with 20 µg/ml of CDDP. Results are expressed as percent of the control value and are the mean ± SD from three independent experiments. ** p-value Ò0.01 vs. 253J C-r NSsh CDDP treated cells, § p-value Ò0.05 vs. 253J C-r NSsh-siNrf2 treated with CDDP, Òp-value Ò0.05 vs 253J YAPsh treated with CDDP.

**Figure 8. Migration of 253J cells**. Wound healing analysis of the migration of 253J, 253J C-r NSsh, 253J C-r NSsh-siNrf2, 253J C-r YAPsh, 253J C-r YAPsh-siNrf2 cells.
Quantification of wound healing was expressed as percent of cell migration and was measured by calculating the reduction in the width of the wound after 24 h and compared to 0 h which is set at 100%. The data of each assay was done from 3 independent experiments and shown as the mean ± SD. ** p-value Ò0.01 vs. 253J C-r NSsh cells, §§ p-value Ò0.01 vs. 253J C-r NSsh-siNrf2, ÒÒ p-value Ò0.01 vs 253J YAPsh.

**Figure 1**

Click here to download high resolution image

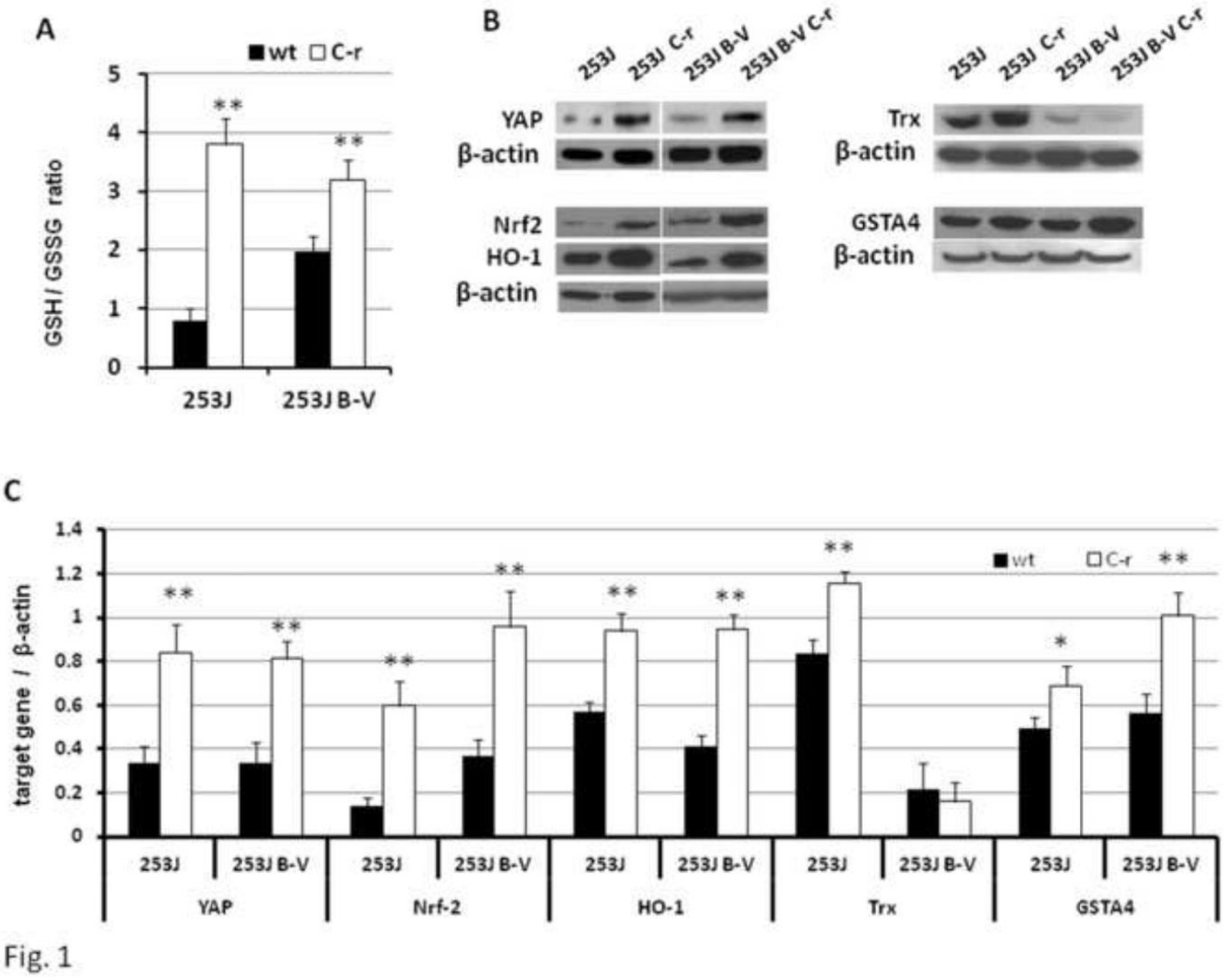


Fig. 1

**Figure 2 new**

Click here to download high resolution image

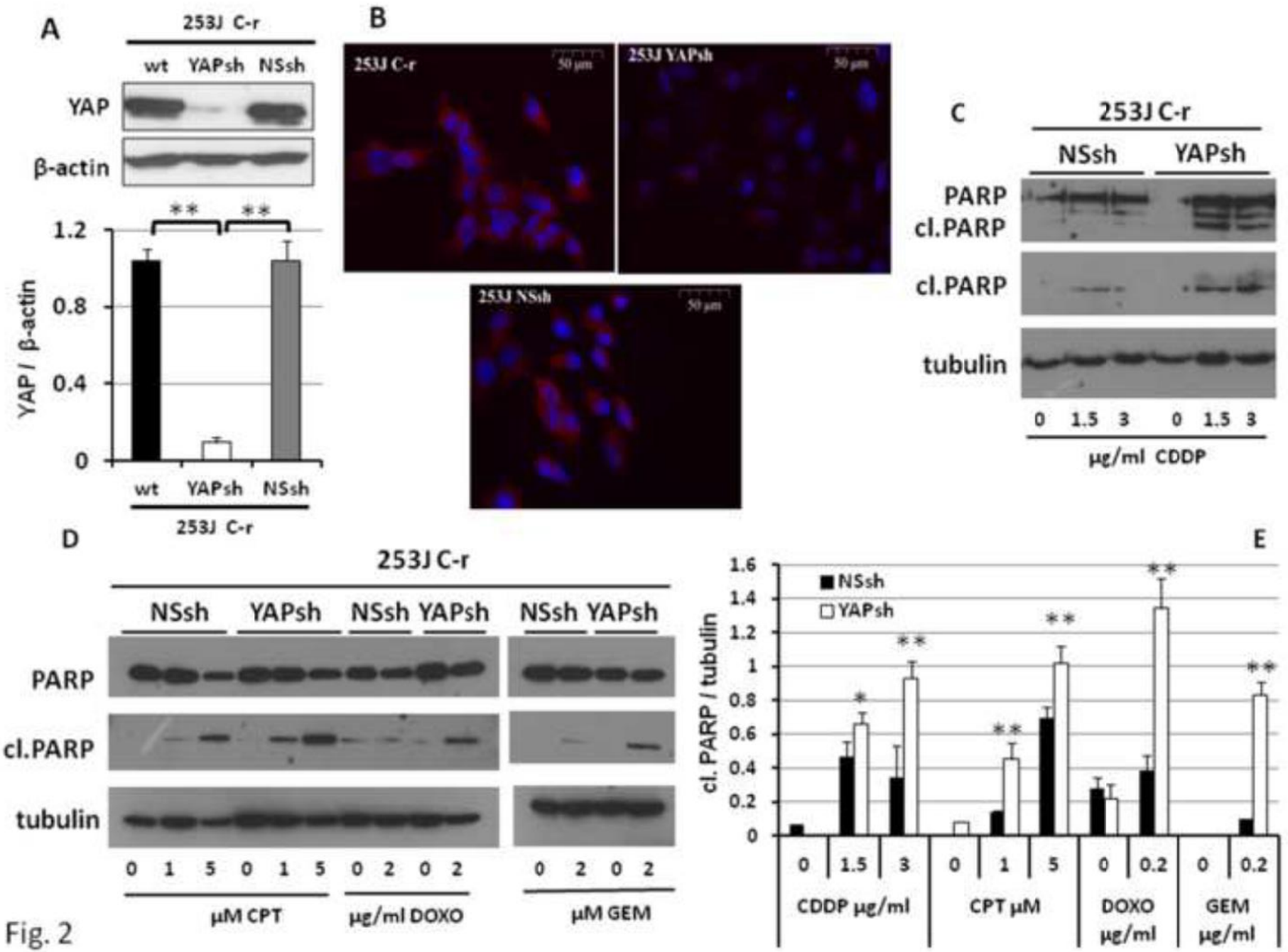


Fig. 2

**Figure 3**
Click here to download high resolution image

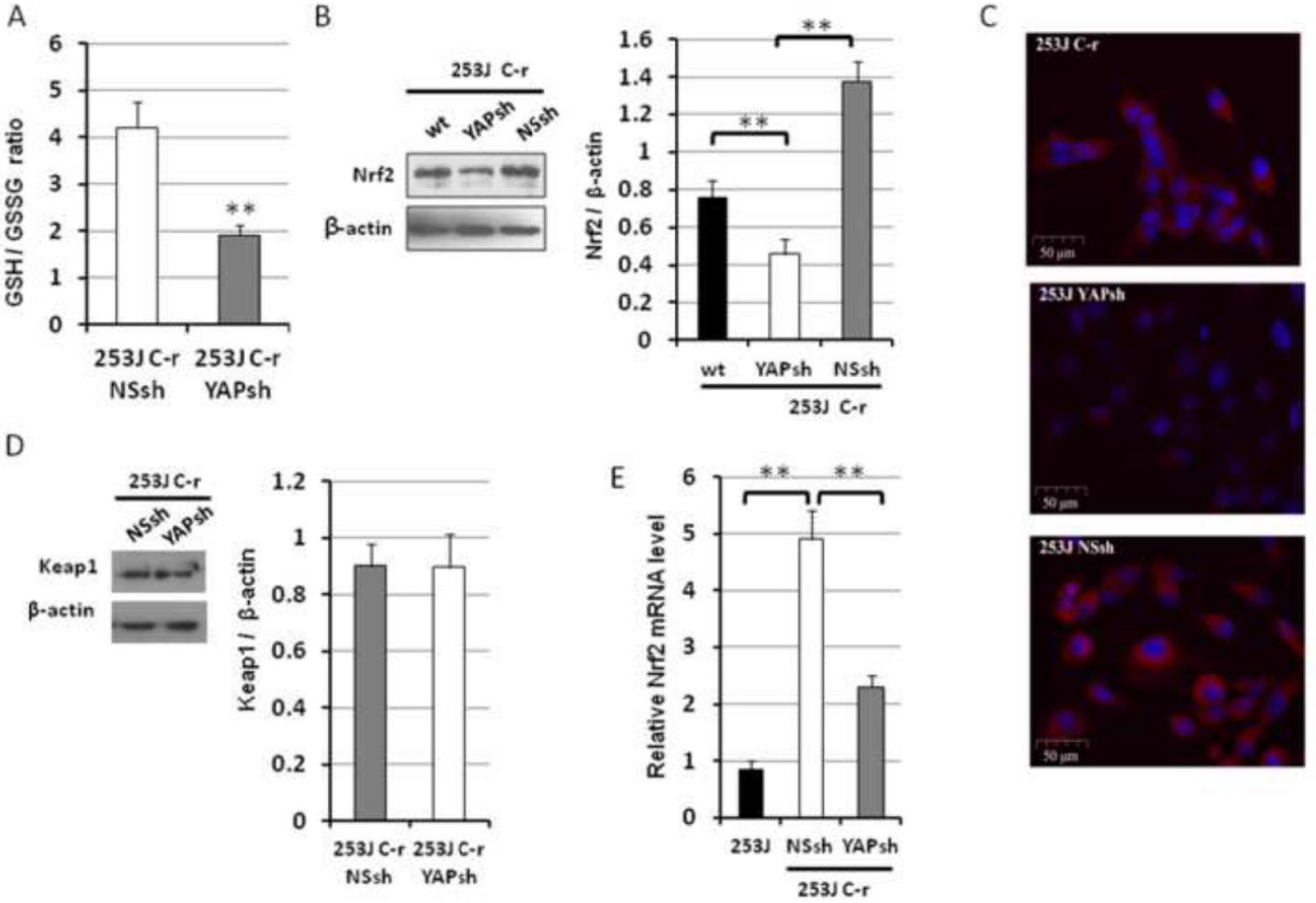


Fig. 3

**Figure 4**

Click here to download high resolution image

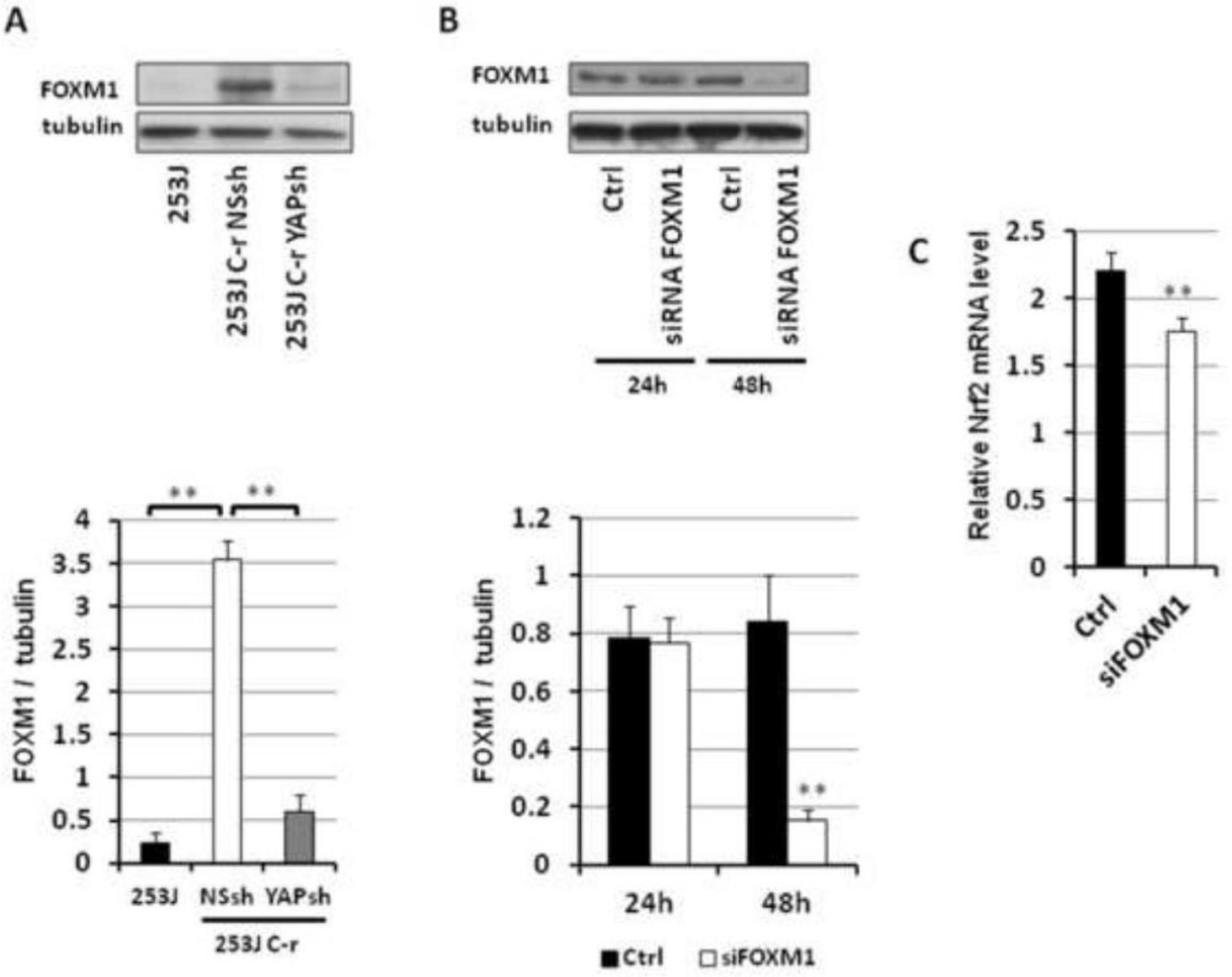


Fig. 4

**Figure 5**

Click here to download high resolution image

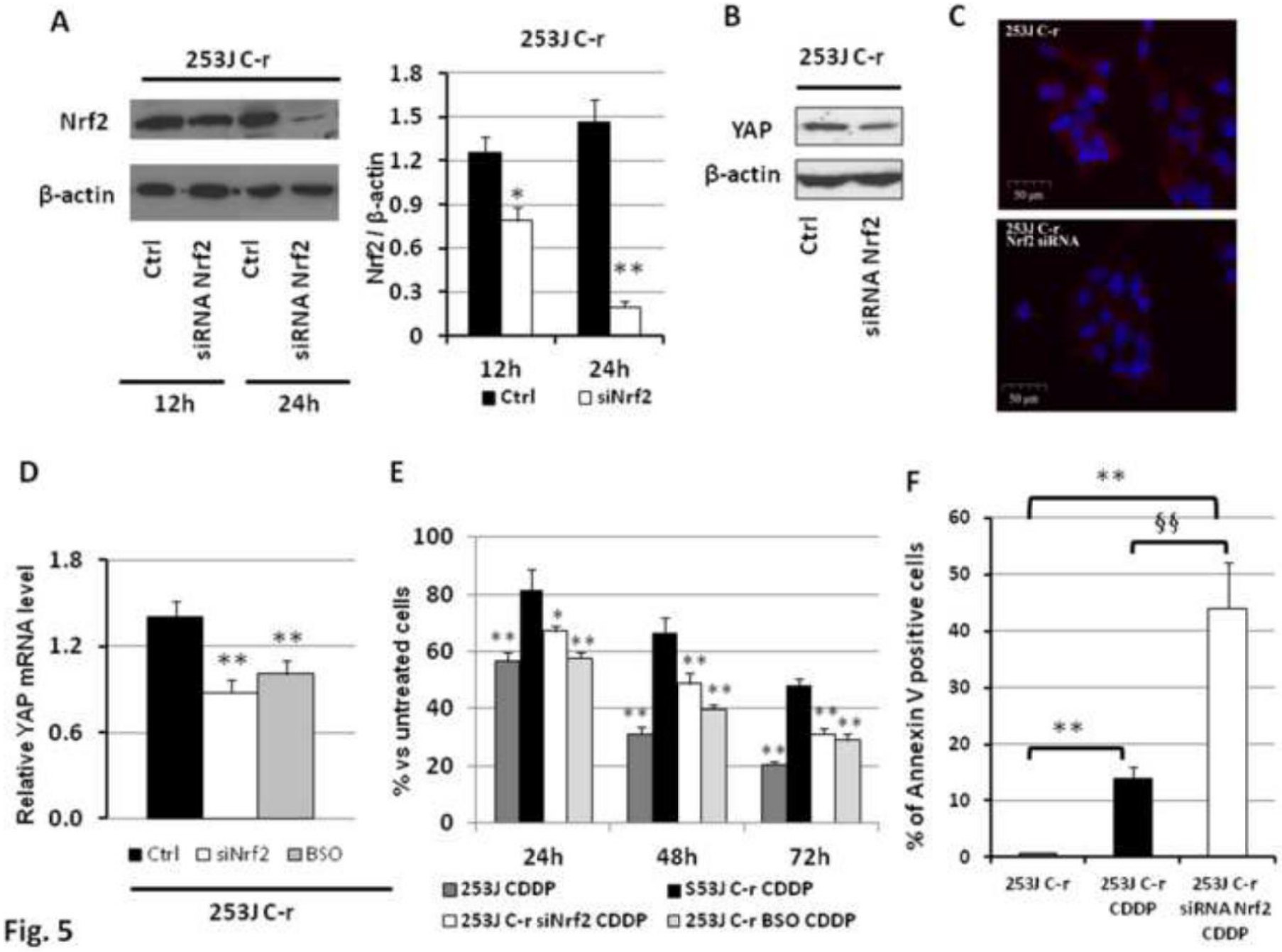


Fig. 5

**Figure 6**

Click here to download high resolution image

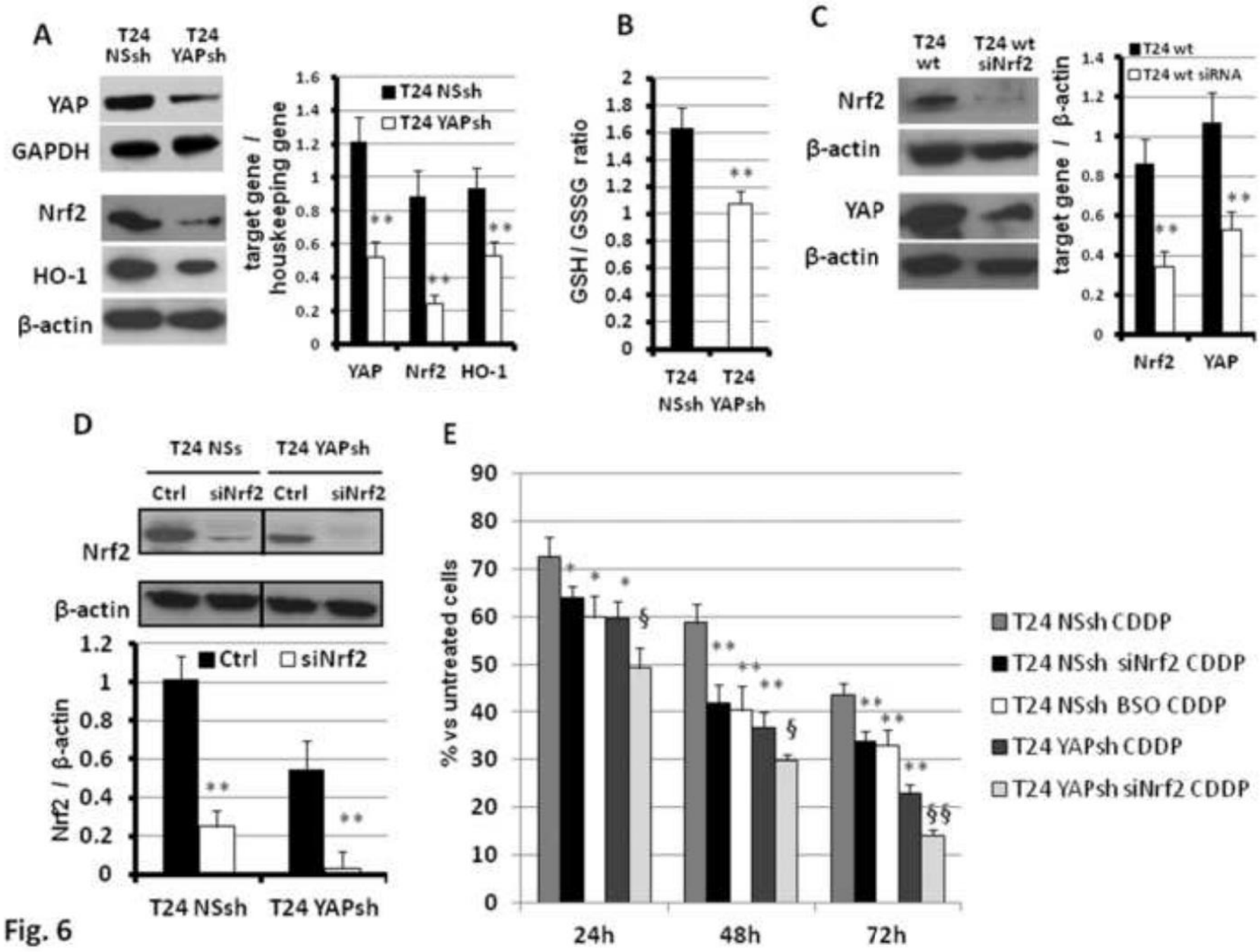


Fig. 6

**Figure 7**

Click here to download high resolution image

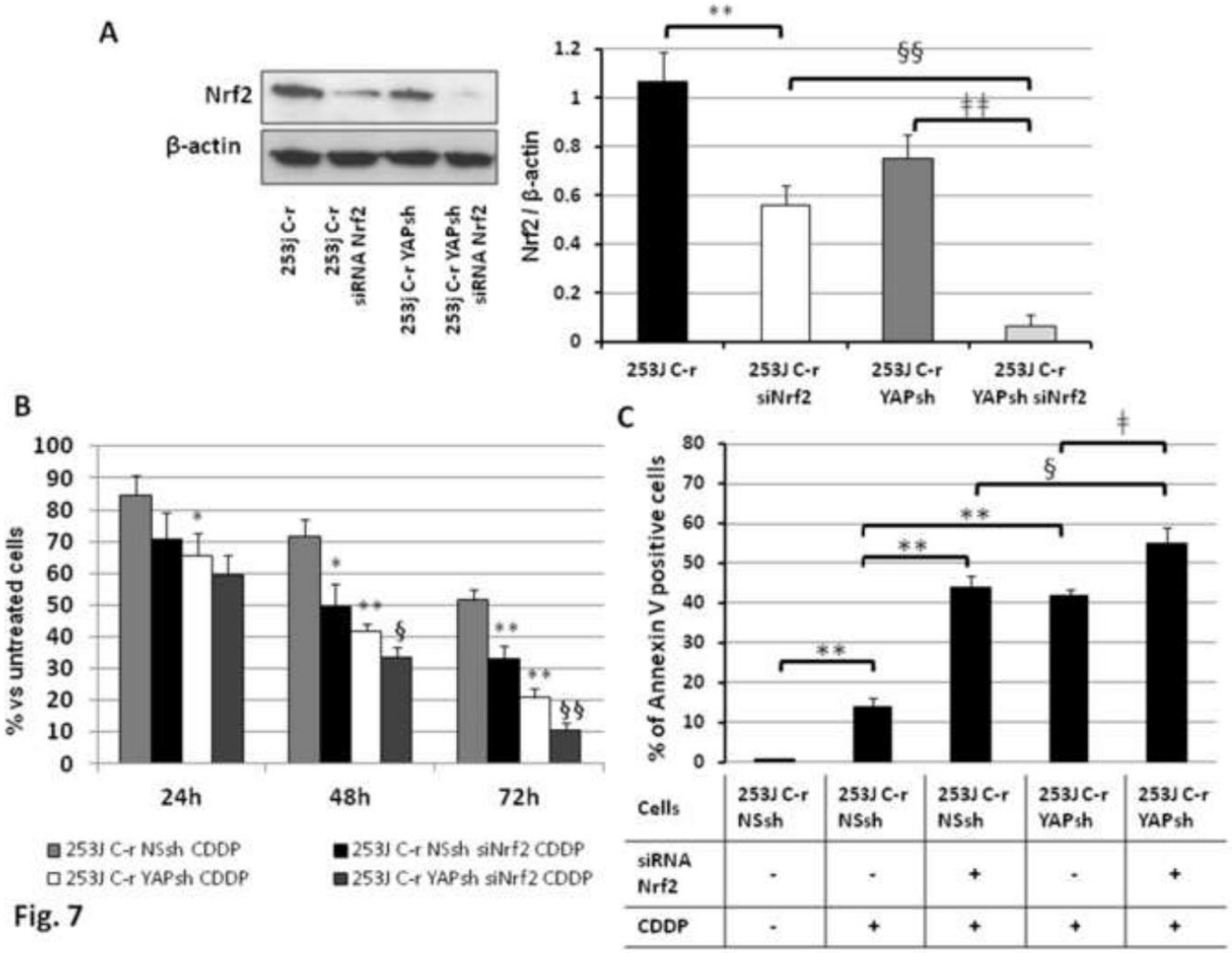


Fig. 7

**Figure 8**

Click here to download high resolution image

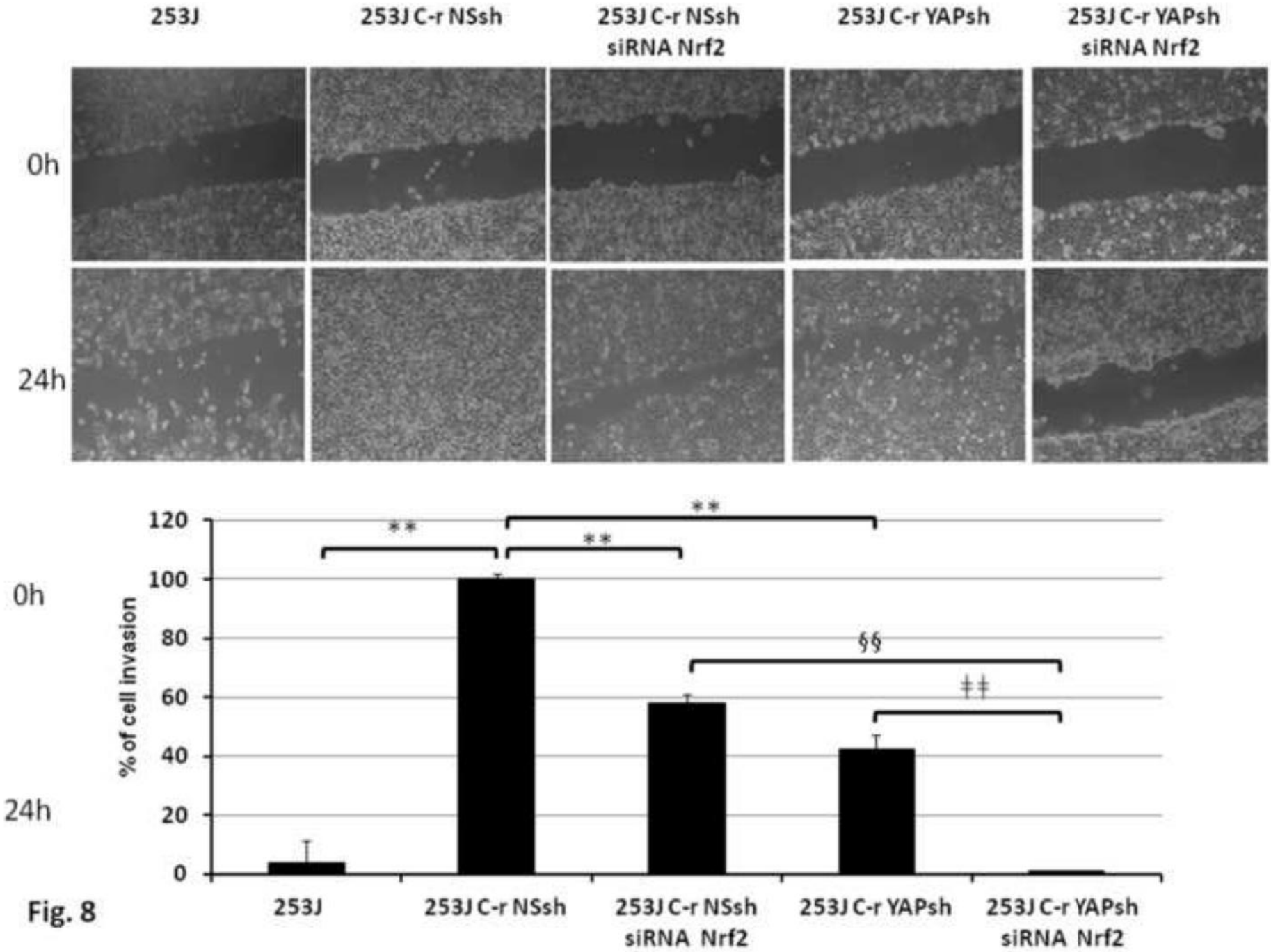


Fig. 8

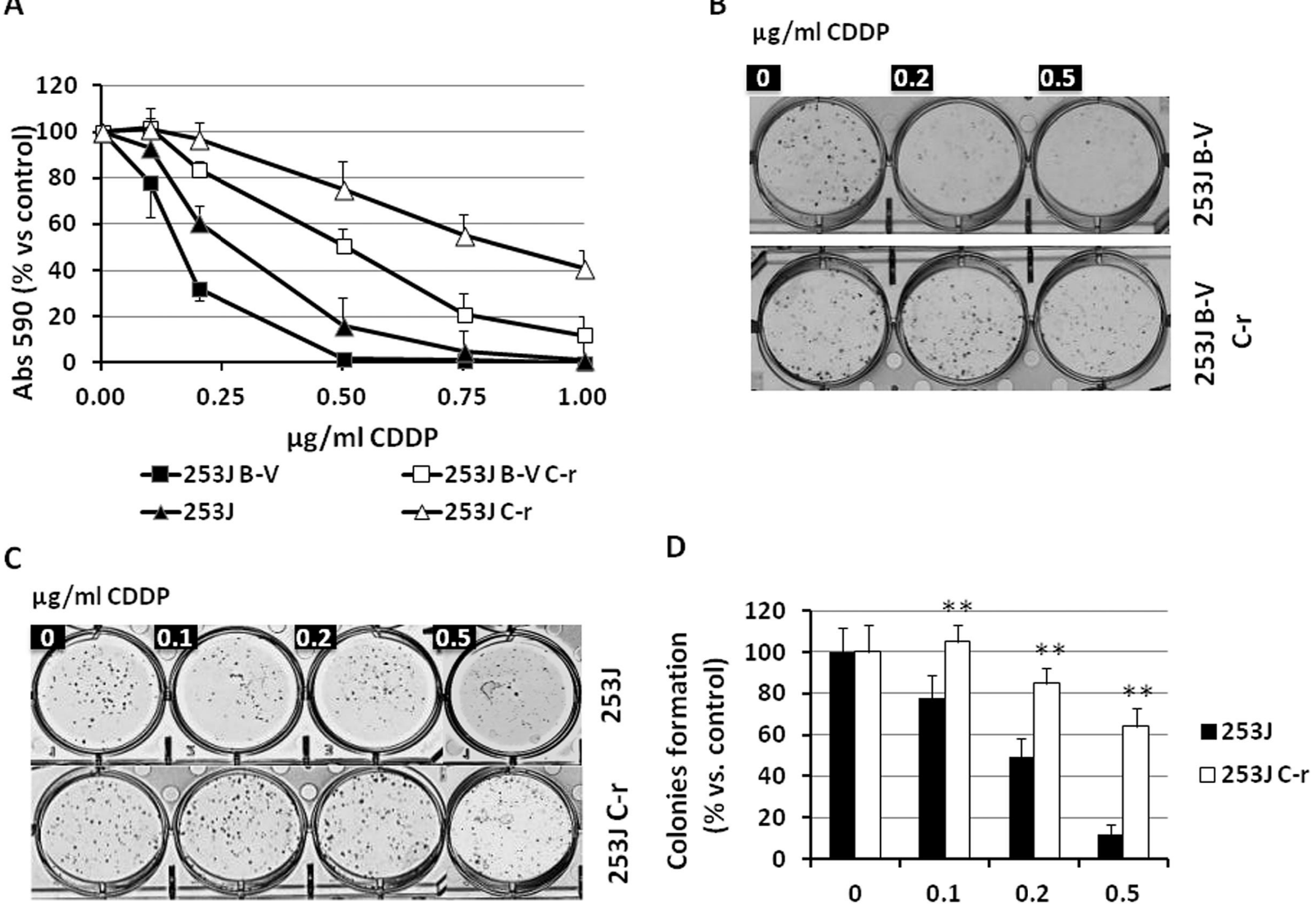


Supplementary data Fig 1